ARTICLE | OPEN ACCESS

Drug Discovery

Author Affiliation:
Biochemistry and Forensic Science Department, Nigeria Police Academy, Wudil, Kano, Nigeria

˚**Corresponding Author**
Godwin O Ihegboro,
Biochemistry and Forensic Science Department, Nigeria Police Academy, Wudil, Kano, Nigeria
Phone number: +2347031149957, +2349072697344
E-mail address: goihegboro@polac.edu.ng

DISCOVERY
SCIENTIFIC SOCIETY

Exploring In silico model to extrapolate the anti-diabetic potential of phytocompounds from *Tapinanthus bangwensis* in type 2-diabetes treatment

Godwin O Ihegboro*, Chimaobi J Ononamadu, Jude Ezeh, Emmanuel C Okoye, Etoro-Abasi Ekanem, Chidimma H Aneke, Divine Imade, Princewwll Odo, Rosemary Jonathan, Hilary Oblia, Marvelous Offuna

ABSTRACT

The study used computational tools to predict the phytocompounds (*Tapinanthus bangwensis)* with potential to ameliorate Diabetes Mellitus. Firstly, two extracts was screened for inhibitory activity; α-amylase (α-A), and α-glucosidase (α-G), and antioxidant capacity; Total antioxidant capacity (TAC), and 2, 2-diphenyl-1-picrylhydrazyl (DPPH) assays. Molecular docking screened the compounds (more active extract) against key target proteins: α-amylase (2QV4), α-glucosidase (2QMJ), pyruvate kinase (4G1N), and glucokinase (3SV4), while using Discovery Studio.to visualize the interactions. SwissADME method was utilized to evaluate ADMET property of the Top-ranked compounds, which include: gastrointestinal tract absorptivity (GITA), blood brain barrier permeability (BBBP), lipophilicity, solubility, glycoprotein substrate permeability (PgSP), bioavailability score (BS), and violation filters (Lipinski, Ghose, Veber, Egan, and Muegge). The result was favorable for the HECF 1 compared to HECF 2, in terms of inhibitory, and antioxidant activity, but substantially inhibits α-amylase activity. The details of the docking scores include: 2QV4 (-3.507 to -6.355, control: -9.085 kcal/mol), 2QMJ (-3.636 to -6.466, control: -8.311 kcal/mol), 4G1N (-3.587 to -6.355, control: -7.016 kcal/mol) and 3SV4 (-3.518 to -7.694, control:-7.081kcal/mol). Diiodotyrosylglycine (compound six), and 1-(-4-Chloro-3-trifluoromethyl) phenyl)-3-(4-hydroxyphenyl) urea (compound one) formed complexes with all the enzymes at different catalytic sites, while the compounds interacted with one or two of the enzymes. All the compounds had BS of 55.0%, and high GITA (except neophytadiene: compound ten). The compounds showed good lipophilic poses (1.43 to 6.92), except compound six (0.85). Three compounds (one, six, and ten) were impermeable to BBB compared to the other compounds. Compound ten served as the only substrate for glycoprotein permeability. Morpholine palmitate (compound thirteen), and compound ten were poorly soluble in aqueous medium. Finally, Compound 1 had no record of violations but others had

one or more violation filters. In conclusion, the study suggests that compound one, and compound six, may be the promising anti-diabetic compounds.

Key words: *Tapinanthus bangwensis*, Molecular docking, Antioxidant, ADME-drug property, Target proteins.

1. INTRODUCTION

Literally, cells require a lot of energy to regulate a good number of biological functions like cell proliferation, cell cycle, and bio-signaling by utilizing specific pathways, including phosphorylation, an ubiquitous metabolic reaction where phosphoyl group (PO_3^{2-}) is transferred to biomolecules for adenosine triphosphate synthesis (Deshpande, 2023). Metabolites (fatty acid, proteins, and ketone bodies) serve as sources of energy to cells. Nevertheless, glucose remains the main energy source, owing to its hydrophilic, tolerability, efficiency, and availability. In a situation, in which glucose uptake exceeds its metabolic rate, a more substantial glucose level is found in circulation, leading to Diabetes Mellitus (DM or hyperglycemia). Also, reactive species can severely damage the islet of Langham (insulin-releasing site), resulting to poor insulin secretion, with more substantial blood glucose concentration (Ihegboro et al. 2020a; Abdul et al. 2025). DM ranks the number three after oncopathy, and cardiomyopathy with minimal death causalities. Diabetic patients face very serious consequences, including limb amputation, cardiomyopathy, retinopathy, hepatopathy, neuropathy, nephropathy and reproductive disorders (Alam et al., 2021). A report posted on the website of the International Diabetes Federation, suggests that between the year 2021 (432 million), and 2045 (783 million), about 351 million more people will be living with DM, with some larger populations between the ages of 20, and 85 years (International Diabetes Federation, 2021; Ononamadu et al., 2024). Sadly, the report indicates that people residing in low-income nations (including Nigeria) will be grossly affected over the next 25 years (Abdul et al., 2025). This underscores the need to intensify efforts to demystify the unwholesome consequences associated with DM. In today's world, synthetic drugs like metfonin, glibenclamide, sulfonylurea, α-glucosidase inhibitor (Acarbose, Miglitol), thiazolidinedione (rosiglitazone, pioglitazone), meglitinides (glinides), bile acid sequestrants (colesevelam) sodium/potassium pump channel, sodium-glucose co-transporters inhibitors (Canagliflozin, Dapagliflozin)), Dopamine-2-agonists (Bromocriptine), DPP-4-inhibitors (gliptins), glycolytic enzymes inhibitors, and carboxylic enzymes inhibitors, are currently being used to regulate glucose homeostasis in diabetic individuals (Chaudhury et al., 2017). Toxicity signs namely: stomach discomforts, bladder cancer, urinary and respiratory tract infections, malabsorption, heart failures, liver diseases, nauseating, and vomiting were reported (Mohiuddin et al., 2019; Ihegboro et al., 2020b). Thus, more research efforts must be invested to promote Phytomedicinal therapy (including African mistletoe: *Tapinanthus bangwensis*) drug discovery and design. African mistletoe, a member of the Loranthaceae family, is an ancestral plant of African origin found in tropical, and subtropical areas. It lives a parasite-host relationship, and synthesizes carbohydrate via the photophosphorylation pathway. The leaf contains match-like flowers with dispersible seeds, which can be dispersed by either birds or wind. *Afomo onisana, Awurusie,* and *Kauchi,* are local names often used by the Yoruba, Igbo, and Hausa, to describe the plant (Ihegboro et al., 2023).

Originally, medicinal plants are used solely as vegetables (nutrition), but currently they are utilized as medicines. Its efficacy lies with the presence of specific natural compounds, which offers substantial therapeutic options for treating numerous ailments, including DM. But uncovering the unique structures of these natural compounds has become very problematic. This led to the advancements in instrumentation, with the design, and development of NMR-MS, LC-MS, GC-MS, HPLC-MS, and computer-aided studies (In Silico) used to elucidate novel compounds in extracts in drug discovery (Ononamadu et al., 2024).

Sincerely, these advanced techniques have helped to reposition drug discovery, with a paradigm shift to in silico studies compared to the routinely used damp chemistry (or experimental studies). It saves time by resolving large numbers of compounds simultaneously, and is cost-effective compared to damp chemistry (Ononamadu et al., 2024). Again, it identifies, and prioritizes potentially active compounds in complex matrix of partial extracts via virtual screening methods. The technique covers both structure-based, and ligand-based methods. However, their use depends on the availability of structural data. For instance, the use of ligand-based method (Pharmacophore model, and quantitative-based model) are only possible, if the ligand molecules are identified without the target structure. But when there are more target data compared to ligands, the structure-based method becomes more suitable, with molecular docking being frequently employed (Meng et al., 2011). Molecular docking, is a first line method that predicts the binding affinity between small molecules (ligands), and protein targets (Safitri et al. 2020). It screens, identifies, and visualizes active compounds from plant extracts before further pharmacological studies (in vivo or cell line). The ligand's position, orientation, and the

conformational binding sites of the protein determines the docking scores (or binding energy) or SILEs (size independent ligand efficiencies score). Molecular studies could be utilized to validate the potential use of medicinal plants as therapeutic agents, providing a platform for experimental research, and drug development (Ahmed et al., 2014; Natarajan et al., 2015). The study investigated the anti-diabetic potential of phytocompounds isolated from *Tapinanthus bangwensis*, by using molecular docking, and ADME-drug likeness models.

2. MATERIALS AND METHODS

2.1. Chemicals/Reagents

Alpha-D-glucopyranoside, n-hexane, Ethyl acetate solvent, Ethanol, Glucosidase, DPPH, Ascorbic acid, ABTS (3-ethylbenzothiazoline-6-sulfonate), potassium persulfate powder, sodium phosphate buffer, dinitrosalicylic acid, acarbose, and starch solution (1%), All the materials are analytical grade.

2.2. Plant Identification and Extraction

The method of Ihegboro et al. (2020a) was used. Previously, the plant was identified as *Tapinanthus bangwensis,* and registered as LUH 4532. The leaves were washed, air-dried (± 28 °C) for five days, and pulverized as powdered mass (500g). It was then dissolved in hexane solvent (1.5L), and left for 48 hours. The filtrate that was obtained was concentrated to form a solid extract (10.5g). The extract was introduced onto a packed column glass containing a mixture of silica gel, and hexane solvent. Setting the flow rate to 5mL/min, the varying concentrations of the eluting solvents (hexane, and ethyl acetate) were utilized to elute the extract. The fractions collected was then resolved into three fractions by considering same retention factors.

2.3. Assessing the In vitro Antioxidant Potency of the extracts

2.3.1. Using the DPPH Test

The method described by Ihegboro et al. (2020a & 2020b) was adopted. It started with preparing different concentrations of the extracts (20 - 100μg/mL). In each concentration, 2mL of DPPH solution (0.1mM) was added, and vortexed vigorously in photophobic room for thirty minutes. The absorbance of the solution, and the positive control (Ascorbic acid) was taken at 517nm. Both the inhibition (%), and mean inhibition concentration (IC_{50}) was determined.

$$DPPH\ inhibition\ (\%) = \frac{Absorbance\ of\ control\ -\ Absorbance\ of\ extract\ x\ 100}{Absorbance\ of\ control}$$

2.3.2. Using the ABTS Test

The method of Rohmah, (2022) was employed. Initially, 5mL of ethanol was used to dissolve 7.1 mg ABTS powder, and 3.5mg potassium persulfate powder separately. Both solutions were incubated for twelve hours in a photophobic room. They were later mixed together, and the volume made up to 25 mL by adding ethanol. An equal volume of the ABTS solution, and the extract (20 - 100μg/mL) was mixed thoroughly. Afterward, the absorbance was taken at 520nm, and converted to inhibition (%), and IC_{50} (from the graph).

$$ABTS\ inhibition\ (\%) = \frac{Absorbance\ of\ control\ -\ Absorbance\ of\ extract\ x\ 100}{Absorbance\ of\ control}$$

2.4. Assessing the extract inhibitory potential on the enzymes

2.4.1. α-Glucosidase Assay

The method by Smita et al. (2018) was used. In a test tube having 0.01M phosphate buffer, 0.25mL 0.5mM pNPG (α -D-glucopyranoside), and 0.1mL α –glucosidase, a 100 μL of the extract was introduced into it, and incubated (± 37 °C) for twenty minutes. This was followed with the addition of 0.1M sodium carbonate solution to stop the reaction. The p-nitrophenol colored product was then measured at 400nm. The percentage inhibition, and mean inhibition concentration was determined.

$$\alpha - G\ (\%) = \frac{Absorbance\ of\ control\ -\ Absorbance\ of\ extract\ x\ 100}{Absorbance\ of\ control}$$

2.4.2. α-Amylase Assay

The protocol as described by Mahnashi, (2022) was adopted. The extract (20 - 100 μg/mL) was put in a test tube, followed by the addition of 200 μL sodium phosphate buffer (0.02M, pH 6.9) together with 20 μL α –amylase, and was incubated (± 25 °C) for ten minutes. Adding a starch solution (1%, 200 μL), the mixture was re-incubated (± 25 °C) for another ten minutes. The test tube was heated for five minutes, and some quantity of water (15 mL). The reaction was stopped with 400 μL DNS reagent (dinitrosalicylic acid). Both the negative control (buffer only), and the positive control (acarbose) were also prepared. The absorbance was taken at 540 nm, and the data obtained were converted to percentage inhibition, while the IC_{50} extrapolated from the graph.

$$\alpha - A\ (\%) = \frac{Absorbance\ of\ control\ -\ Absorbance\ of\ extract\ x\ 100}{Absorbance\ of\ control}$$

2.5. Identification of the compounds in the extract

The Vignesh et al. (2022) method was utilized. Liquid-chromatography-Mass Spectroscopy (LC-MS: W2998 PDA model) was used to identify the phytocompounds. Firstly, a filtrate was prepared by dissolving the extract in hexane solvent, and filtered through a polytetrafluoroethylene membrane filter (pore size: 0.45 μm). The filtrate (10 μL) was then injected into the machine with the aid of a syringe. Two mobile phase solvents namely: solvent A (0.1% formic acid in water) and solvent B (0.1% formic acid in acetonitrile) were used. At the beginning, the gradient ratio 95:5 A/B was held for one minute, which was then changed to 5:95 for fifteen minutes, and returned to 95:5 for twenty minutes. The technique's condition (LC) includes: flow rate: 1.0 mL/min @ 25 °C; Sample rate (10 points/sec), PDA detector (210-400 nm) and Resolution (1.2 nm), while the MS are: fragmentation voltage (125 V), nebulizer gas pressure (45 psi), probe temperature (600 °C) and flow rate (10 mL/min).

2.6. Antidiabetic Prediction of the compounds (In Silico model)

The method described by Ononamadu and Ibrahim, (2021) was used. The details of the HP Ellitebook B40 G3 laptop system used are as follows: Intel (R), core i5, 15-6300U CPU @ 2.40GHz – 2.50GHz, 8.0GB RAM, memory spacing (256GB), and operating system (64-bit). In addition, the MOE software 2015, Microsoft Excel 2016; RCSB protein Data Bank (PDB) database, and Pubchem database were utilized.

2.6.1. Preparation of the Target proteins (Enzymes)

The identities of the target proteins are: α-amylase (PDB ID: 2QV4), α-glucosidase (PDB ID: 2QMJ), glucokinase (PDB ID: 3SV4) and pyruvate kinase (PDB ID: 4G1N) were for the molecular docking. The 3D structures of the target proteins, including the co-crystals were downloaded from the (https://www.rcsb.org/) database (accessed on 11th October, 2024), and saved as a PDB file.

2.6.2. Preparation of the compounds (Ligands):

The 3D structural data of the sixteen compounds were downloaded from the (https://pubchem.ncbi.nlm.nih.gov/) database (accessed on 10th October, 2024), and saved as a spatial data file (SDF). They were washed, protonated, and minimized using open Babel software, before being transformed to a PDBQT format.

2.6.3. Docking simulation

The molecular studies was conducted using MOE 2015, while the docking scores were read using the London dG/GBVI/WSA, and saved in a MDB format. The binding interaction was visualized with the Discovery Studio. All through the simulation process, both the docking exhaustiveness (DE), and grid point distance (GPD) was maintained at 0.375 Å and 20, respectively.

2.6.4. Drug-likeness study

SwissADME method was employed to evaluate the physicochemical properties of the top-ranked docked compounds. The properties considered are as follows: gastrointestinal tract absorption (GITA), blood-brain barrier permeability (BBBP), glycoprotein permeation (Pgp), Bioavailability scores, Lipophilicity, solubility, and violation filters (Lipinski, Ghose, Veber, Egan, and Muegge rules of 5 (RO5).

Statistical Analysis

The data obtained were converted to Mean± S.E.M using the Statistical package for Social Science (SPSS version 23.0), with significance set at p < 0.05.

3. RESULTS

3.1. Antioxidant effect of the extracts and Ascorbic Acid

The result showed that the reference drug (Ascorbic acid) inhibits the radicals (2, 2-diphenyl-1picylhydrazyl, DPP*) more substantially ($p < 0.05$) compared to the extracts. The result showed that the extracts exhibited similar inhibitory activity, but no significant difference exists. In like manner, the reference drug inhibits the activity of the ABTS radicals more substantially ($p < 0.05$) compared to the extracts. Although, the HECF 1 extract showed a higher inhibition level compared to the HECF 2 extract, there was no significant difference in the activity (Figure 1).
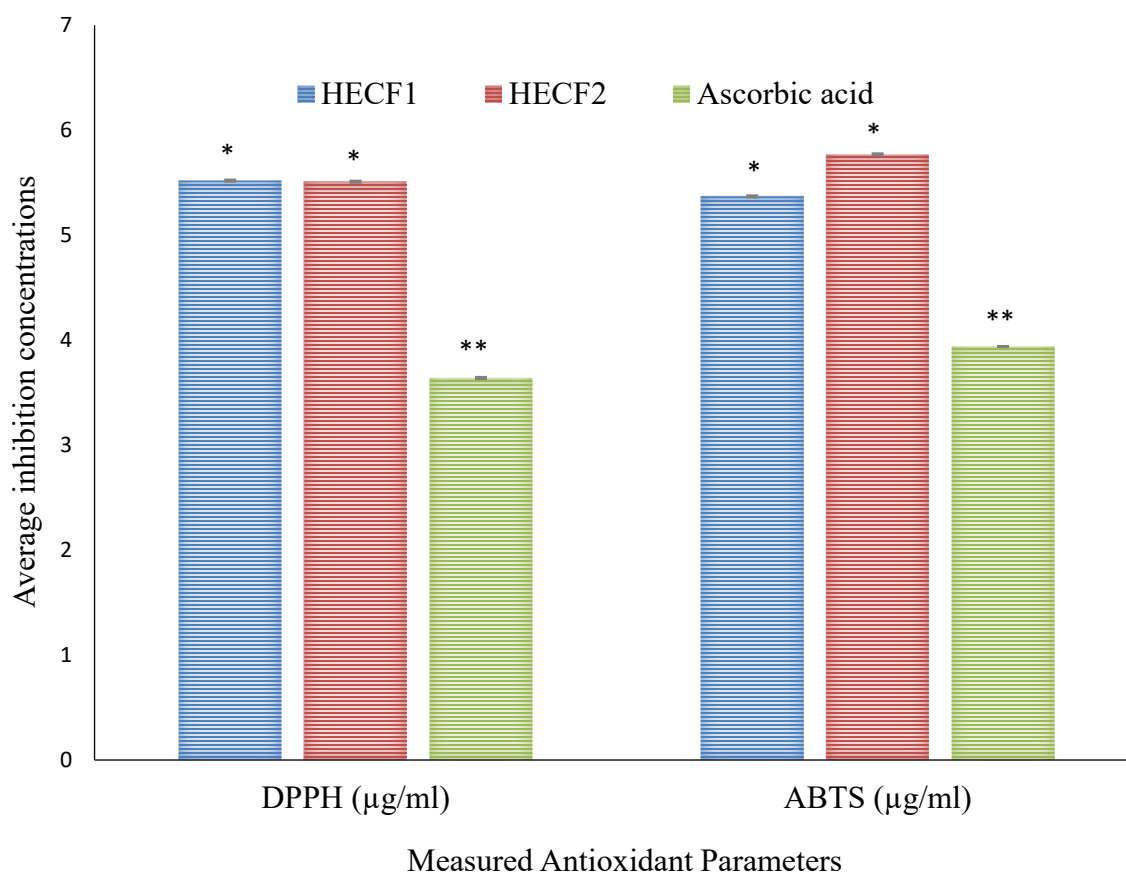

Figure 1: Showing the average inhibition concentrations (IC$_{50}$) of both the extracts and ascorbic acid (Reference drug) using DPPH and ABTS Assays.

3.2. Anti-α-A and Anti-α-G Activity (In vitro)

The inhibitory activity of the reference drug (Acarbose) was more substantial ($p < 0.05$) against α-amylase and α-glucosidase activity compared to the extracts (Figure 2). The result showed that the HECF 1 inhibits α-amylase activity in a more substantial manner ($p < 0.05$) compared to the HECF 2 extract. Also, the HECF 1 extract showed a higher inhibitory effect against α-glucosidase compared to the HECF 2 extract, but no significant difference exists (Figure 2).

3.3. Docking and Binding interaction between the ligands and binding sites of α-amylase

In Table 1, the result showed that the Docking energies of the compounds were between -3.507 to -6.355 kcal/mol compared to the control (-9.085 kcal/mol). All the compounds had a SILE score within the range of -2.013 to -2.774 compared to the control (-2.7303), respectively. The result showed that 1-(-4-Chloro-3-trifluoromethyl) phenyl)-3-(4-hydroxyphenyl) urea (compound 1) binds at the Arg 195, and Asp 300 amino acid residues of the target protein (*α-amylase*) via hydrogen bonding. Neophytadiene (compound 10) showed a

π bond interaction with the Trp 59 amino acid residue. Diiodotyrosylglycine (compound 6) interacted with the protein's catalytic sites (Asp 197, and Asp 300 amino acid residues) via hydrogen bonding. In contrast, methimazole (compound 8) showed binding interaction with His 299, Arg 195, and Asp 197 amino acid residues of the enzyme. The result showed that the control (α-D-glucopyranoside) had a better binding interactions via hydrogen bonding compared to the compounds. Conversely, an ionic bond interaction exists at Glu 233 amino acid residue, and a π bond at the Tyr 62 amino acid residue {Table 2, Figure 3 (a – e)}.
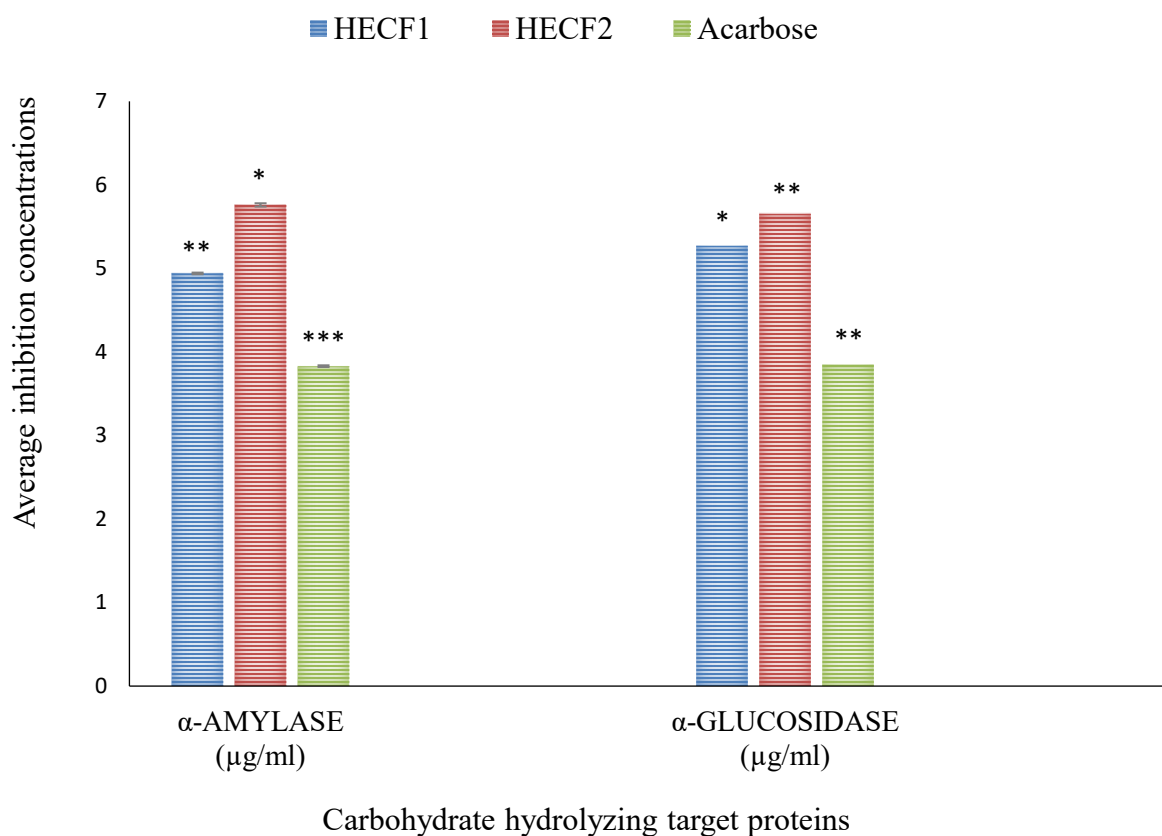

Figure 2: Showing the inhibition level of the extracts and acarbose against α-amylase and α-glucosidase activity.

Table 1: Showing the results of the docking energies and SILE scores of the compounds

S/N	CID	Identified Compounds	Docking energy	SILE scores
1	25221150	1-(-4-Chloro-3-trifluoromethyl) phenyl)-3-(4-hydroxyphenyl) urea	-5.3641	-2.1221
2	102013209	1-Hydroxyphosphirene	-3.5069	-2.3137
3	5366161	3,7,11,15-tetramethyl-2-hexadecene	-5.8720	-2.3904
4	89706674	4-Pent-1-en-2-ylthiomorpholine	-4.6281	-2.2542
5	644019	Cannabidiol	-5.9336	-2.3163
6	129715761	Diiodotyrosylglycine	-5.2367	-2.1649
7	11086	Ethanone, 1-(2-aminophenyl)	-4.3164	-2.1633
8	1349907	Methimazole	-4.0190	-2.2418
9	27946	1-Aminopyrrolidine	-3.7358	-2.1824
10	10446	Neophytadiene	-5.9013	-2.4024
11	558410	Pyrrolidine-(3-methyl-3-butenyl)	-5.0672	-2.5396
12	8987	Sodium diethyl dithoicarbamate trihydrate	-4.2207	-2.2618

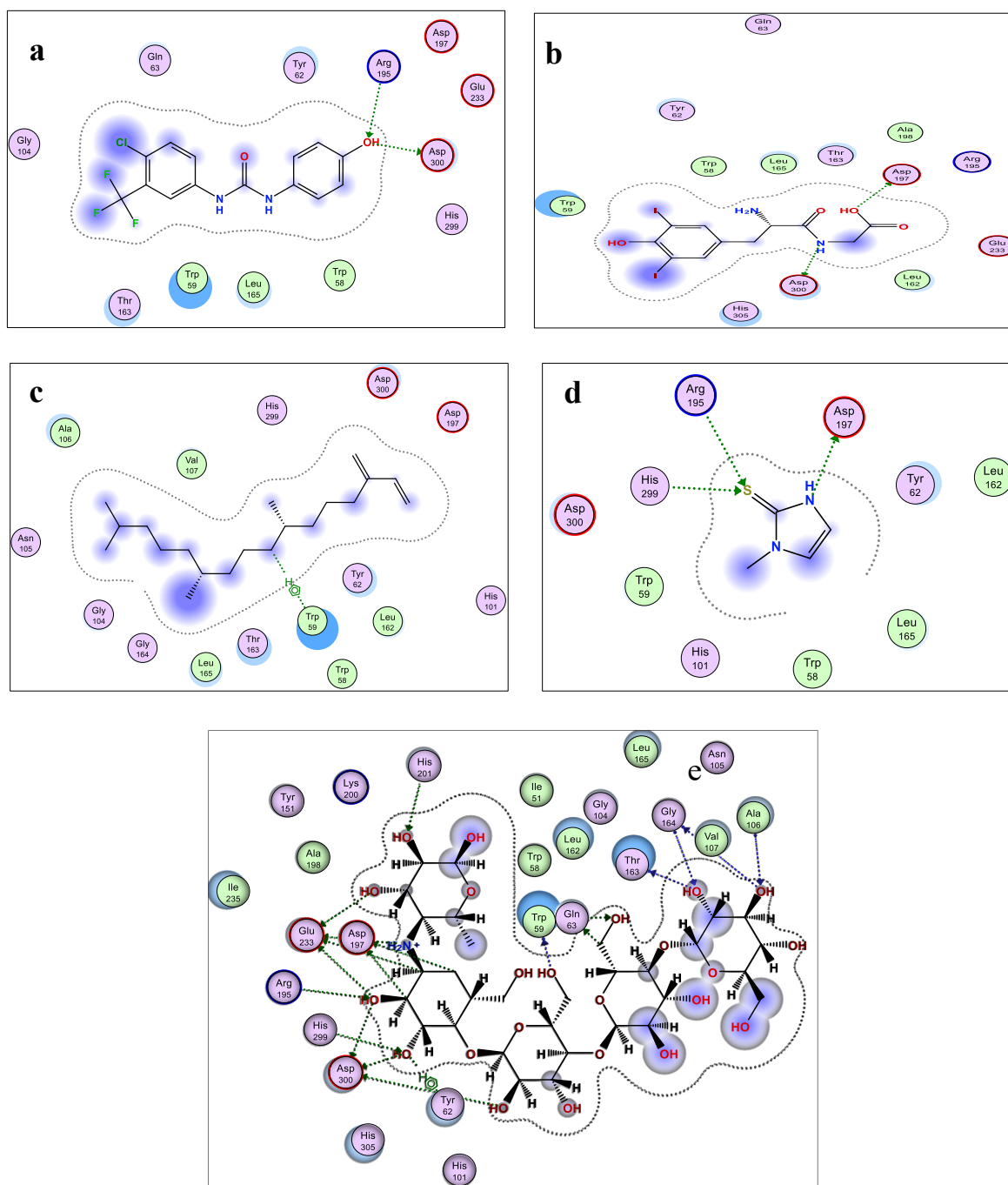| 13	129727309	Morpholine palmitate	-6.3550	-2.4494
14	5281	Octadecanoic acid	-5.7788	-2.3525
15	3862902	1-cyclohexenylboronic Acid	-3.8919	-2.0132
16	6449799	Bromomesaconic acid	-4.3630	-2.1867
		α-D-glucopyranoside (control)	-9.0854	- 2.7303

Figure 3: The 2D representation of the interactions between the selected compounds (ligands) and the target protein receptor (α-amylase) (a) 1-(-4-Chloro-3-trifluoromethyl) phenyl)-3-(4-hydroxyphenyl) urea (b) diiodotyrosylglycine (c). Neophytadiene (d). Methimazole (e). Control

Table 2: Showing the binding interactions between the Top-ranked compounds (ligands) and α-Amylase binding sites.

S/N	Selected Compounds	Amino acid Interaction/Distance
1	1-(-4-Chloro-3-trifluoromethyl) phenyl)-3-(4-hydroxyphenyl) urea	Asp 300[x] (2.81), Arg 195[x] (3.38)
6	Diiodotyrosylglycine	Asp 197[x] (2.77), Asp 300[x] (3.03)
8	Methimazole	Asp 197[x] (2.99), Arg 195[x] (4.04), His 299[x] (3.43)
10	Neophytadiene	Trp 59[y] (4.26)
	α-D-glucopyranoside (control)	Thr 163[x] (2.64), Gly 164[x] (3.17), Gln 63[x] (2.41), Asp 300[x] (3.25), Trp 59[x] (2.73), Asp 197[x] (2.96), Ala 106[x] (2.86), His 201x (2.82), Arg 195[x] (2.96), His 299[x] (2.93), Tyr 62[y] (3.62), Glu 233[z] (3.31)

Keys: x, y and z indicates H-Bond, pi-Bond and ionic bond respective, while the values in the bracket indicates the interaction distance.

3.4. Docking and Binding interaction between the compounds and α- glucosidase binding sites

The docking energies (compounds: –3.636 to –6.416 kcal/mol, control: -8.311 kcal/mol), and the SILE scores (compounds: -2.113 to -3.167, control: -2.671) are shown in Table 3. The result revealed that compound one showed interaction at the Asp 327, Met 444, and Asp 203 catalytic sites of the enzyme (α- glucosidase) with hydrogen bond as the stabilizing force. The binding affinities of compound six were at these catalytic sites of the enzyme (Asn 449, Arg 526, Asp 542, and Met 444 amino acid residues) via hydrogen bonding. Bromomesaconic acid (compound sixteen) formed hydrogen bond complexes with His 600, Asp 542, and Met 444 amino acid residues of the protein. From the result, a hydrogen bonding interaction exists between Ethanone, 1- (2-aminophenyl) (compound seven), and the Asp 327, and His 600 catalytic sites of the protein. Conversely, compound seven interacted via π bonding with Tyr 299 amino acid residue of the target protein. Acarbose (control) showed a more substantial binding interaction with the catalytic sites of the enzyme (eight different amino acid residues) via hydrogen linkages. Acarbose also formed an ionic bond interaction with the Asp 542 amino acid residue of the target protein {Table 4, Figure 4 (a – d)}.

Table 3: Showing the results of the docking energies and SILE scores of the compounds.

S/N	CID	Identified Compounds	Docking energy	SILE scores
1	25221150	1-(-4-Chloro-3-trifluoromethyl) phenyl)-3-(4-hydroxyphenyl) urea	-5.6572	-2.2381
2	102013209	1-Hydroxyphosphirene	-3.6364	-2.3991
3	5366161	3,7,11,15-tetramethyl-2-hexadecene	-6.0644	-2.4688
4	89706674	4-Pent-1-en-2-ylthiomorpholine	-4.6544	-2.2670
5	644019	Cannabidiol	-6.4160	-2.5046
6	129715761	Diiodotyrosylglycine	-5.7476	-2.3761
7	11086	Ethanone, 1- (2- amino phenyl)	-4.3972	-2.2038
8	1349907	Methimazole	-4.2926	-2.3944
9	27946	1-Aminopyrrolidine	-4.0319	-2.3554
10	10446	Neophytadiene	-6.0672	-2.4699
11	558410	Pyrrolidine, N-(3-methyl-3-butenyl)	-4.2150	-2.1125
12	8987	Sodium diethyl dithoicarbamate trihydrate	-4.4053	-2.3607
13	129727309	Morpholine palmitate	-6.2969	-2.4270
14	5281	Octadecanoic acid	-5.9046	-2.4037
15	3862902	1-cyclohexenylboronic Acid	-4.3783	-2.2648
16	6449799	Bromomesaconic acid	-4.7865	-2.3989
	445421	α-Acarbose (control)	-8.3110	-2.6706

Table 4: Result showing the binding interactions between the Top-ranked compounds (ligands) and α-glucosidase binding sites.

S/N	Compounds with interactions	Amino acid Interaction/Distance
1	1-(-4-Chloro-3-trifluoromethyl) phenyl)-3-(4-hydroxyphenyl) urea	Asp 327[x] (3.30), Met 444[x] (3.39), Asp 203[x] (2.89)
6	Diiodotyrosylglycine	Asn 449[x](3.87), Asp 542[x] (2.97), Met 444[x] (3.69), Arg 526[x] (3.02)
7	Ethanone, 1- (2- amino phenyl)	Asp 327 [x](2.82), His 600 [x] (3.11), Tyr 299[y] (3.66)
16	Bromomesaconic acid	Met 444[x] (3.91), Asp 542[x] (2.93), His 600[x] (3.61)
	α-Acarbose (control)	Thr 205[x] (3.41), Asp 203[x] (2.92), Met 444[x] (3.55), Asp 542[x] (2.57), Asp 443[x] (3.06), Asp 327[x] (2.47), Arg 526[x] (2.80), His 600[x] (2.97), Asp 542[z] (2.83)

Keys: x, y and z signifies Hydrogen Bond, pie Bond and ionic bond respectively, while the values in the bracket stands for the interaction distance.
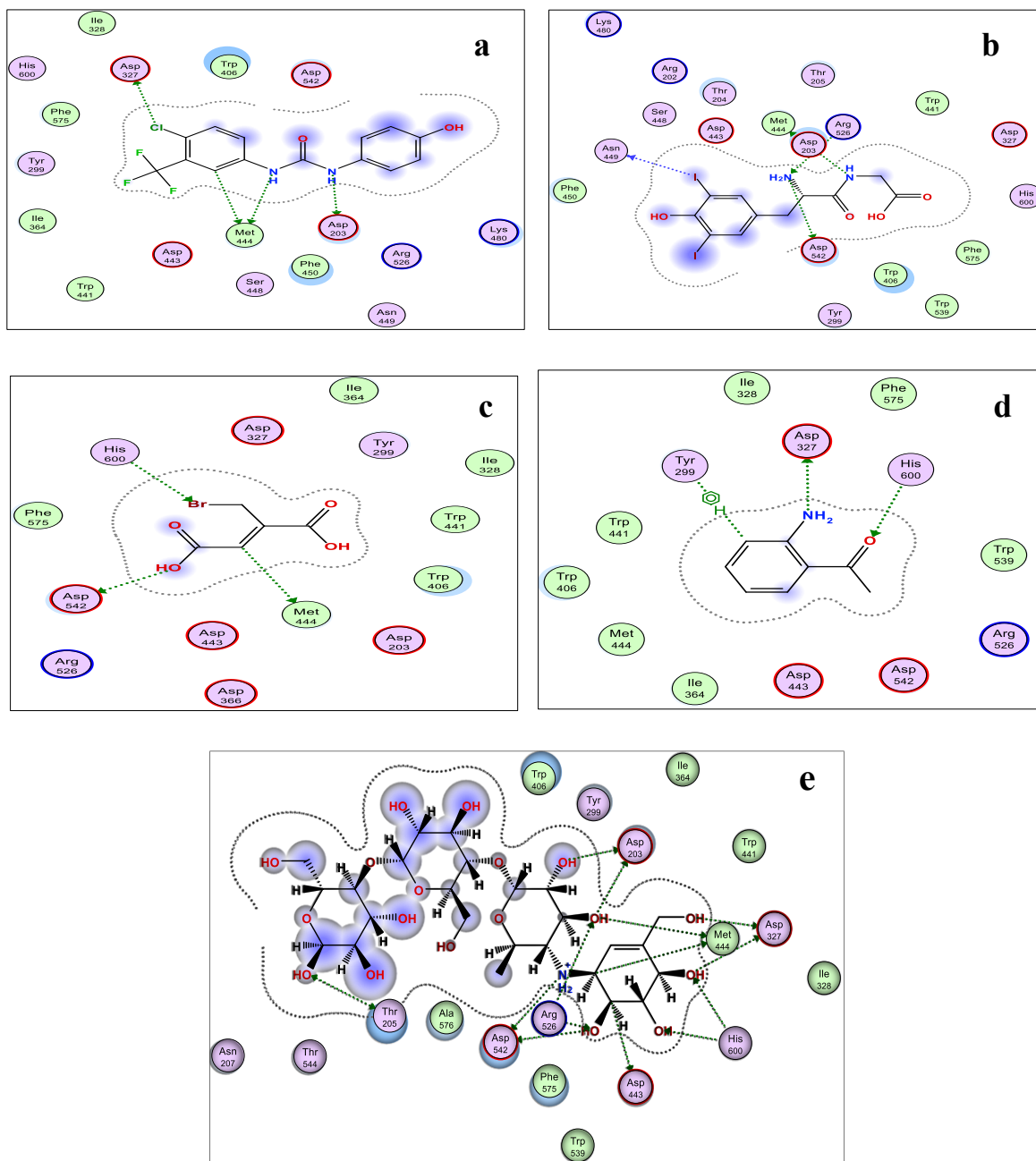

Figure 4. The 2D representation of the interaction between the selected compounds (ligands) and the target protein receptor (α-glucosidase) **(a)** 1-(-4-Chloro-3-trifluoromethyl) phenyl)-3-(4-hydroxyphenyl) urea **(b)** diiodotyrosylglycine **(c)** Bromomesaconic acid **(d)** Ethanone, 1- (2- amino phenyl) **(e)**. Control
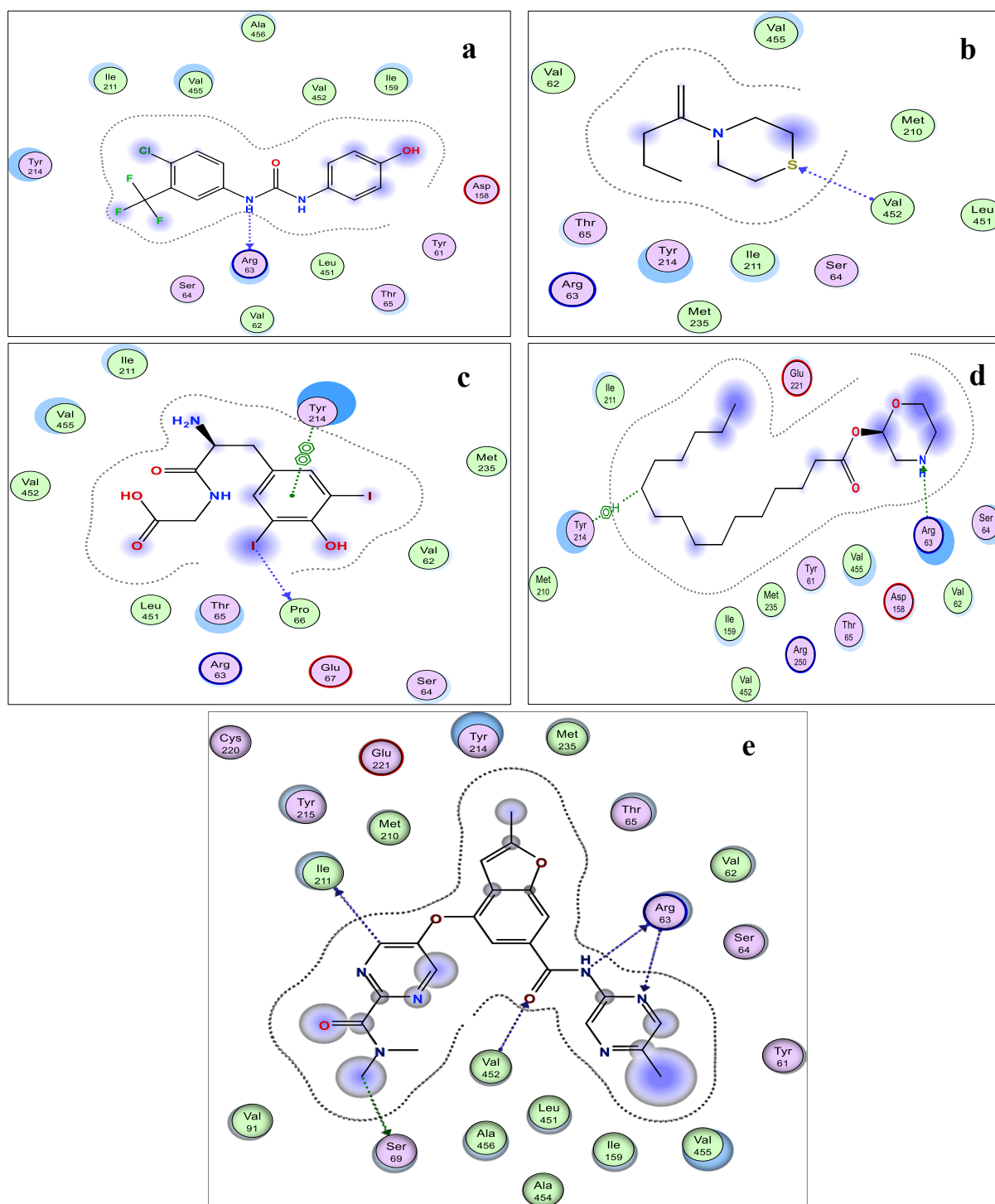
Figure 5. The 2D representation of the interaction between the selected compounds (ligands) and glucokinase receptor **(a)** 1-(-4-Chloro-3-trifluoromethyl) phenyl)-3-(4-hydroxyphenyl) urea **(b)** 4-Pent-1-en-2-ylthiomorpholine. **(c)** Diiodotyrosylglycine. **(d)** Morpholine palmitate **(e)**. Control

3.5. Docking and Binding interaction between the compounds and Glucokinase binding sites

According to Table 5, the docking energies of the compounds was in the range of -3.518 to -7.694 kcal/mol, while the SILE score ranges between -2.1739 to -2.9655. Nevertheless, the docking energy for nerigliatin (control) was higher compared to the other compounds, except morpholine palmitate (compound thirteen). The result revealed that compound one interacted with the protein's catalytic site at Arg-63 amino acid residue via a hydrogen bond, whereas 4-Pent-1-en-2-ylthiomorpholine (compound four) interacted at the Val 452

amino acid residue via a hydrogen linkage. The result showed that compound six interacted at the Pro 66 amino acid residue via a hydrogen bond, while also interacting with Tyr 214 amino acid residue via a π bond linkage. Moreover, the interaction between morpholine palmitate (compound thirteen), and Arg 63 amino acid residue was stabilized by a hydrogen bond, as well as showing interaction at the Tyr 214 amino acid residue via a π bond. Nerigliatin (control) showed a hydrogen bond interaction at the Arg 63, Ile 211, Ser 69, and Val 452 amino acid residues of the target protein [Table 6, Figure 5 (a –d)].

Table 5: Showing the results of the docking energies and SILE scores of the compounds

S/N	CID	Identified compounds	Docking energy	SILE scores
1	25221150	1-(-4-Chloro-3-trifluoromethyl) phenyl)-3-(4-hydroxyphenyl) urea	-6.4387	-2.5472
2	102013209	1-Hydroxyphosphirene	-3.5176	-2.3208
3	5366161	3,7,11,15-tetramethyl-2-hexadecene	-7.2242	-2.9409
4	89706674	4-Pent-1-en-2-ylthiomorpholine	-5.2348	-2.5497
5	644019	Cannabidiol	-6.6004	-2.5766
6	129715761	Diiodotyrosylglycine	-6.1902	-2.5590
7	11086	Ethanone, 1- (2- amino phenyl)	-4.3375	-2.1739
8	1349907	Methimazole	-4.1945	-2.3396
9	27946	1-Aminopyrrolidine	-3.9245	-2.2927
10	10446	Neophytadiene	-6.9163	-2.8156
11	558410	Pyrrolidine, N-(3-methyl-3-butenyl)-	-4.9043	-2.4580
12	8987	Sodium diethyl dithoicarbamate trihydrate	-4.3492	-2.3307
13	129727309	Morpholine palmitate	-7.6942	-2.9655
14	5281	Octadecanoic acid	-5.7788	-2.3525
15	3862902	1-cyclohexenylboronic Acid	-3.8919	-2.0132
16	6449799	Bromomesaconic acid	-4.3630	-2.1867
	46916694	Nerigliatin (control)	-7.0807	- 2.5005

Table 6: Result showing the binding interactions between the Top-ranked compounds (ligands) and glucokinase binding sites

S/N	Selected compounds	Amino acid Interaction/Distance
1	1-(-4-Chloro-3-trifluoromethyl) phenyl)-3-(4-hydroxyphenyl) urea	Arg 63[x] (2.96)
4	4-Pent-1-en-2-ylthiomorpholine	Val 452[x] (3.65)
6	Diiodotyrosylglycine	Pro 66[x] (3.47),Tyr 214[y] (3.72)
14	Morpholine palmitate	Arg 63[x] (3.20),Tyr 214[y] (4.13)
	Nerigliatin (control)	Arg 63[x] (3.02), Ile 211[x] (3.49), Ser 69[x] (3.03), Val 452[x] (3.64).

Keys: x and y indicates H-Bond and pi-Bond respective, while the values in the bracket indicates the interaction distance.

3.6. Docking and Binding interaction between the compounds and the Pyruvate kinase binding sites

Table 7 revealed that the docking energy (-7.016 kcal/mol) for 1-Deoxynojirimycin (control) was higher compared to the compounds (-3.507 to - 6.355 kcal/mol), while also having a higher SILE score (-3.4172) compared to the compounds (-2.0913 to -2.961). The result as shown in Table 8, Figure 6 (a –d) indicated that compound one showed interaction at the Asp 354, Asn 318, Lys 311 and Arg 445 amino acid residues, and was sustained by hydrogen bond. In a like manner, compound four showed a hydrogen bonding interaction with the Arg 445 amino acid residue of the target protein. The compound six showed molecular interactions at these specific catalytic sites of the target protein (Asn 318, Arg 319, and Cys 31) via a hydrogen bonding. In contrast, compound eight formed a hydrogen cross-bridge interaction with Asn 318, Met 30, and Arg 445 amino acid residues. The result showed that 1-Deoxynojirimycin (control) binds to the catalytic sites of the enzyme at Leu 353, and Tyr 390 amino acid residues via a hydrogen bond, but exhibited a я bond interaction at the Leu 394 amino acid residue of the target protein.
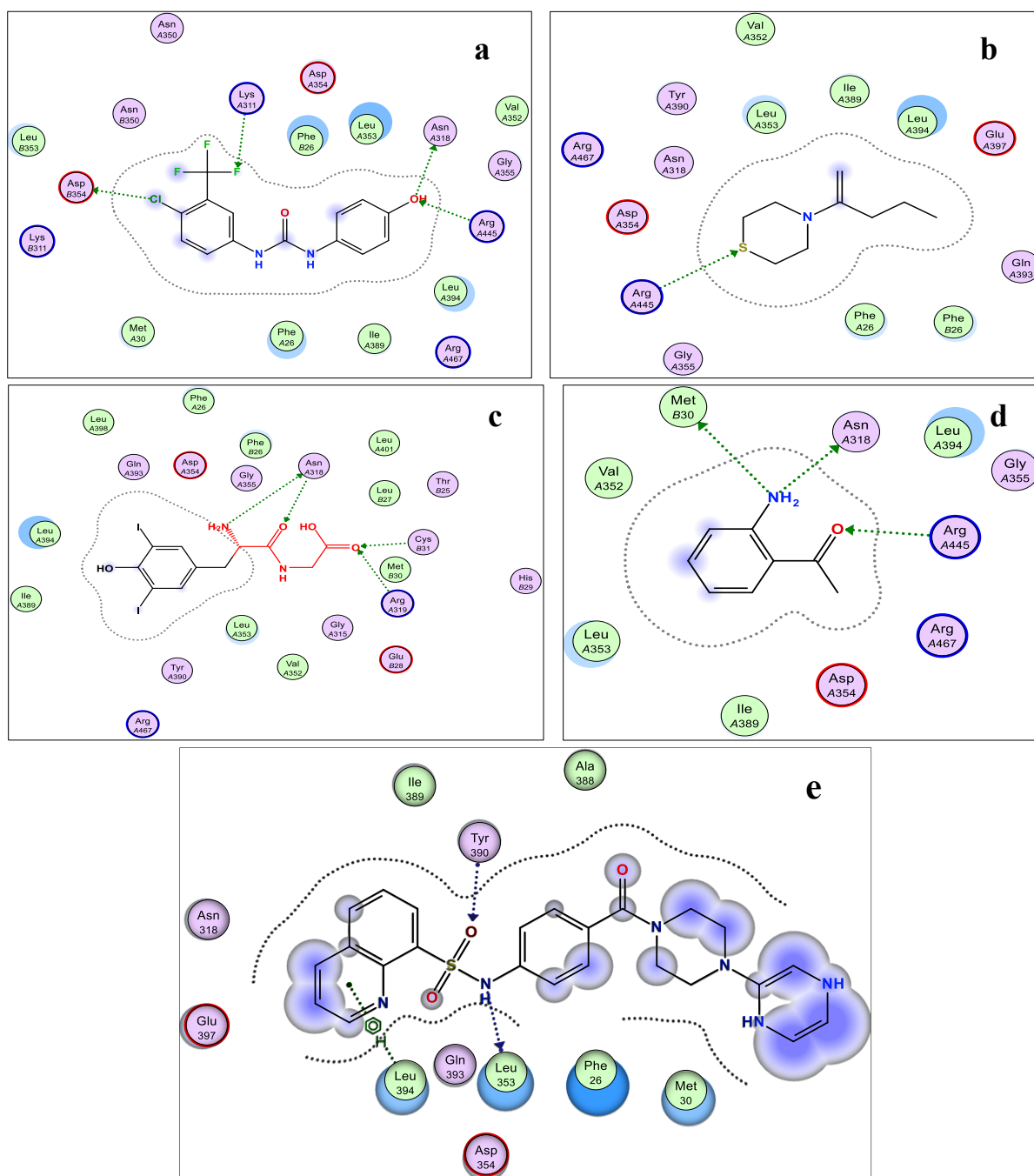
Figure 6: The 2D representation of the interaction between the selected compounds and the target protein receptor (pyruvate kinase) (a) 1-(-4-Chloro-3-trifluoromethyl) phenyl)-3-(4-hydroxyphenyl) urea (b) 4-Pent-1-en-2-ylthiomorpholine (c) diiodotyrosylglycine (d) Ethanone-1-(2-aminophenyl) (e). Control.

Table 7: Showing the results of the docking energies and SILE scores of the compounds (ligands).

S/N	CID	Identified compounds	Docking energy	SILE scores
1	25221150	1-(-4-Chloro-3-trifluoromethyl) phenyl)-3-(4-hydroxyphenyl) urea	-5.3641	-2.1221
2	102013209	1-Hydroxyphosphirene	-3.5069	-2.3137
3	5366161	3,7,11,15-tetramethyl-2-hexadecene	-5.8720	-2.3904
4	89706674	4-Pent-1-en-2-ylthiomorpholine	-4.6281	-2.2542
5	644019	Cannabidiol	-5.9336	-2.3163

6	129715761	Diiodotyrosylglycine	-5.2367	-2.1649
7	11086	Ethanone, 1-(2-aminophenyl)	-4.3164	-2.1633
8	1349907	Methimazole	-4.0190	-2.2418
9	27946	1-Aminopyrrolidine	-3.7358	-2.1824
10	10446	Neophytadiene	-5.9013	-2.4024
11	558410	Pyrrolidine, N-(3-methyl-3-butenyl)-	-5.0672	-2.5396
12	8987	Sodium diethyl dithoicarbamate trihydrate	-4.2207	-2.2617
13	129727309	Morpholine palmitate	-6.3550	-2.4494
14	5281	Octadecanoic acid	-5.7788	-2.3525
15	3862902	1-cyclohexenylboronic Acid	-3.8919	-2.09132
16	6449799	Bromomesaconic acid	-4.3630	-2.1867
	29435	1-Deoxynojirimycin (control)	-7.0161	- 3.4172

Table 8: Result showing the binding interactions between the Top-ranked compounds (ligands) and pyruvate kinase binding sites.

S/N	Compounds with interactions	Amino acid Interaction/Distance
1	1-(-4-Chloro-3-trifluoromethyl) phenyl)-3-(4-hydroxyphenyl) urea	Asp 354[x] (3.22), Asn 318[x] (3.12), Lys 311[x] (3.36), Arg 445[x] (3.07)
4	4-Pent-1-en-2-ylthiomorpholine	Arg 445[x] (4.36)
6	Diiodotyrosylglycine	Asn 318[x] (3.30), Arg 319[x] (3.57), Cys 31[x] (2.60)
7	Ethanone,1-(2-aminophenyl)	Asn 318[x] (2.98), Met 30[x] (4.46), Arg 445[x] (3.54)
	1-Deoxynojirimycin (control)	Leu 353[x] (2.71), Tyr 390[x] (2.41), Leu 394[y] (3.77)

Keys: x and y signifies Hydrogen Bond and pie-Bond respectively, while the values in the bracket indicates the interaction distance.

Table 9: The Physicochemical properties of the six Top-ranked compounds from the results of the Docking simulation

S/N	Selected Compounds	Lipophilicity	Solubility (log$_{10}$S)	GIA	BBBP	PgpS	Lipinski	Ghose	Veber	Egan	Muegge	Bioavailability scores
1	1-(-4-Chloro-3-trifluoromethyl) phenyl)-3-(4-hydroxyphenyl) urea	3.77	Moderately soluble	High	No	No	0	0	0	0	0	0.55
4	4-Pent-1-en-2-ylthiomorpholine	2.29	Soluble	High	Yes	No	0	0	0	0	1	0.55
6	Diiodotyrosylglycine	0.85	Very soluble	High	No	No	0	1	0	0	0	0.55
7	Ethanone, 1-(2-aminophenyl)	1.43	Soluble	High	Yes	No	0	2	0	0	1	0.55
10	Neophytadiene	6.92	Poorly soluble	Low	No	Yes	1	1	1	1	2	0.55
13	Morpholine palmitate	5.1	Poorly soluble	High	Yes	No	0	0	1	0	2	0.55

Keys: GITA = Gastrointestinal absorption, BBBP = Blood Brain barrier permeation, PgpS = glycoprotein substrate Permeability, Lipophilicity score (consensus log$_{10}$ P0/w).

3.7. The ADME Drug property of the Top-ranked compounds

The result showed that compound ten had the highest lipophilicity score (6.99), while compound 6 exhibited the least lipophilicity score (0.85). The other compounds had lipophilicity scores in the range of 1.4 to 5.1. Compound six showed a high solubility, whereas compound one was moderately soluble. Both compound four, and compound seven were found to be soluble compared to compound ten and compound thirteen, which showed poor solubility (Table 9). All the compounds were highly absorbed in the gastrointestinal

tract (GIT) except compound ten. The result showed a high probability that compound four, compound seven, and compound thirteen to be transported through the blood-brain barrier. The result showed that it was only compound ten that served as a substrate for glycoprotein permeability (Table 9). The bioavailability score was the same for all the compounds (55.0%). Compound one showed no violation filter (Lipinski, Ghose, Veber, Egan, and Muegge), but other compounds had one or more violation filters (Table 9).

4. DISCUSSION

Molecular docking and ADME-Drug likeness model was used to predict the antidiabetic potential of phytocompounds isolated from *Tapinanthus bangwensis*. Today, many ailments challenging human existence arise due to the problems of antioxidant imbalance. In this instance, a more substantial therapeutic option would be to consume food rich in antioxidants such as phytochemicals, pharmaceuticals, and minerals (Ale 2020; Ihegboro et al. 2022). Previously, several analytical approaches were required to validate an extract's antioxidant activity. In contrast, studies have shown that at least two approaches may be employed to establish the antioxidant potential of plant extract or biomolecules (Chaves et al. 2020). The result showed that the extracts has antioxidant capacity to scavenge the presence of both DPP* and ABTS radicals, respectively. But the HECF 1 extract exhibited a higher antioxidant activity compared to the HECF 2. This result is in tandem with an earlier published work (Ihegboro et al. 2019).

A lot of therapeutic strategies are currently in use, in managing postprandial hyperglycemia. But inhibiting the activity of α-amylase (α-A) and α-glucosidase (α-G) was considered the most effective (Ihegboro et al. 2022). The present result shows that the extracts potentially inhibit the activity of these enzymes. Nevertheless, the effect was more substantial against the activity of α-amylase compared to the α-glucosidase (Ihegboro et al., 2020a & 2020b).

Docking score/energy measures the degree of binding affinity between ligands and the target protein's amino acid residues (Iheagwam et al. 2019). A report credited to Qui et al., (2011), they highlighted that compounds that interacts with the catalytic sites of α-A at Asp 300, and Asp 197 amino acid residues, could be a potent α-A inhibitor. The result showed that compound one and compound six interacted at these amino acid residues compared to the other compounds. This suggests that the substantial inhibition of α-A, may be due to the effect of these two compounds. Moreover, compound one and compound seven (Ethanone 1-(2-aminophenyl) interact with α-glucosidase at the Asp 203 and Asp 327 amino acid residues comparable to acarbose (Mustafa et al. 2022). The result agrees with a published report by Ibrahim et al. (2017).

The glucokinase activity is enhanced when specific substances (called activators) binds to the allosteric sites of the enzyme, and stimulates the efflux of insulin from the islet of Langham. Thus, reduces glucose concentration in the blood, which improves glucose homeostasis, and glycemic control (Yixin et al. 2022). In their article, they submitted that the activation of the enzyme occurs at these catalytic sites (Arg 63, Ile 211, Ser 69, Val 452, Met 210, Tyr 214, Pro 66, His 218, Cys 220, Arg 250, Leu 451, and Ala 456), depending on the enzyme type (Yixin et al. 2022). The result showed that only nerigliatin activated glucokinase activity compared to the other compounds, by forming a hydrogen bond at these catalytic sites (Arg 63, Ile 211, Ser 69, and Val 452 amino acid residues) of the target enzyme.

In Pankaj et al. (2021) report, they established that N-(4-[[4-(pyrazine-2yl) piperazin-1-yl] carbonyl} quinoline-8-sulfonamide, NZT) (positive control) forms complexes with pyruvate kinase catalytic sites (Tyr 390, Asp 354, Leu 353, Lys 311) in the presence of hydrogen bond, while forming hydrophobic bond interaction at the Leu 394, and Met 30 amino acid residues of the protein (Pankaj et al. 2021). The control (1-Deoxynojirimycin) showed a similar level of binding interactions (Tyr 390, Leu 353, and Leu 394) as NZT. The present result showed that compound one interacts at the Asp 354, and Lys 311 binding sites of the protein. Conversely, the binding affinity of compound seven was at the Met 30 amino acid residue of the target enzyme. The current result suggests that pyruvate kinase activity, could be well inhibited by compound one compared to the other compounds.

For a compound to be approved as a good candidate for drug design, it must pass through pharmacological, pharmacokinetic and safety tests (Ononamadu and Ibrahim, 2021). Lipophilicity measures the degree at which a compound dissolves in a lipophilic medium (lipid). Studies suggest that within a lipophilic range from 0-5, a compound has the tendency to be translocated across lipid-bound membranes, thereby improving their availability to the target sites (Arnott and Planey, 2012; Daina et al. 2017; Savjani et al. 2012). The result showed that the all compounds had a high lipophilic score, except compound six (0.85). But the lipophilic score of compound ten (6.69), and compound thirteen (5.1) was found to be above the lipophilic range. The result agrees with the study conducted by Ononamadu and Ibrahim, (2021). In contrast, compound ten and compound thirteen were poorly soluble in aqueous medium compared to the other compounds, despite having a high bioavailability score (55.0%), which may affect absorption into the bloodstream.

To avoid central nervous system (CNS) toxicity, the body devices specific mechanisms, avoiding drugs (or substances) from being transported across the brain-barrier (Abbott, 2004). The presence of drug in the brain causes severe adverse neurological effects. Looking at the result, compounds four, compound seven, and compound thirteen showed potential as CNS toxicants (Ononamadu and Ibrahim, 2021).

Glycoprotein permeation is a co-transport carrier protein that facilitates the movement of drugs (substrates) from the plasma or tissue back into the GIT domain (Finch and Pillians, 2014). The result revealed that only compound ten showed capacity for glycoprotein permeability. The purpose of computing violation filters is to predict a compound's uniformity (Daina et al. 2017). All the compounds show at least one or more violation filters except compound one that had no violation filters.

5. CONCLUSION

The use of plant as medicines over synthetic drugs in treating ailments, including Type 2-diabetes cannot be over-emphasized, which underscores the importance of natural products (phytocompounds) in drug design and development. In today world, in silico studies offer a better option compared to experimental studies. This study used computational tools (Molecular simulation and ADMET-drug likeness model) to predict the anti-diabetic potential of phytocompounds isolated from *Tapinanthus bangwensis*. The result revealed that the HECF 1 extract showed a more substantial inhibitory effect against α-amylase (α-A), and antioxidant potential compared to the HECF 2 extract. Furthermore, the result showed that compound one, and compound six exhibited favorable docking energy, and binding interaction at the different catalytic sites of the target proteins compared to the other compounds. The ADMET analysis was essentially favorable for the two compounds. In conclusion, the two compounds may be promising reference candidates for drug development. This research further recommends that the two compounds should be investigated for in vivo and molecular studies.

Ethical Approval
In this article, as per the plant regulations followed in the Biochemistry and Forensic Science Department, Nigeria Police Academy, Wudil, Kano, Nigeria; the authors observed the anti-diabetic potential of phytocompounds from *Tapinanthus bangwensis*. The ethical guidelines for plants & plant materials are followed in the study for observation, identification & experimentation.

Informed Consent
Not applicable.

Conflicts of interests
The authors declare that they have no conflicts of interests, competing financial interests or personal relationships that could have influenced the work reported in this paper.

Data and materials availability
All data associated with this study are herein presented.

REFERENCES

1. Abbott NJ. Prediction of blood brain barrier permeation in drug discovery from in vivo, in vitro and in silico models. Drug discovery Today Tech 2004;1(4):407-416.
2. Abdul S, Ahsan J, Dilber UO, Liker O, Khalid M, Yasir W. Genetics of diabetes and its complication: a comprehensive review. Diabetol metab syndr 2025;17:185
3. Ahmed D, Kumar V, Sharma M and Verma A. Target guided isolation, in-vitro antidiabetic, antioxidant activity and molecular docking studies of some flavonoids from Albizzia Lebbeck Benth. bark. BMC complementary and alternative Med. 2014;14(1):1-3.

4. Alam S, Hassan MK, Neaz S, Hussain N, Hossain MF, Rahman T. Diabetes mellitus insights from epidemiology, Biochemistry, risk factors, diagnosis, complications and comprehensive management. Diabetology 2021;12(2):36-50.

5. Ale E. Assessment of antioxidant properties of N-Hexane extract of *Morinda lucida* as a link to its pharmacological actions. Pharmacy & Pharmacology International Journal, 2020; 8(3):174–178.

6. Arnott JA, and Planey SL. The influence of lipophilicity in drug discovery and design. Expert opiin. Drug Discov 2012;7(10): 863-875.

7. Chaudhury A, Duvoor C, Reddy-Dendi VS, Kraleti S, Chada A, Ravilla R, Marco A, Shekhawat NS, Montales MT, and Kuriakose K. Clinical Review of Antidiabetic Drugs: Implications for Type 2 Diabetes Mellitus Management. Front. Endocrinol 2017;8:6.

8. Chaves N, Antonio S, and Juan CA. Quantification of the antioxidant activity of plant extracts: Analysis of sensitivity and hierarchization based on the method used. Antioxidant 2020;9(1):76

9. Daina A, Michielin O, Zoere V. Swiss-ADME: a free web tool to evaluate pharmacokinetics drug-likeness and mechanical chemistry friendliness of small molecules. Sci Rep 2017;7:42717.

10. Deshpande OA. Biochemistry textbook. 2023.

11. Finch A, and Pillians P. P-glycoprotein and its role in drug-drug interactions. Aust prescr 2014; 37: 137-139.

12. Ibrahim A, Onyike E, Nok AJ and Umar IA. Combination of Gymnemia sylvestre and Combetum micranthum methanol leaf extract produced synergistic hypoglycaemic activity in Alloxan diabetic mice. Saudi J. Med. Pharm 2017;3(11A):1188-1199.

13. Iheagwan FN, Ogunlana OO, Ogunlana OE, Isewon I, Oyelade J. Potential anti-cancer Flavonoids isolated from Caesalpinia bonduc young twigs and leaves: Molecular docking and in silico studies. Bioinformatics. Biol. Ins.t 2019;13:1-16

14. Ihegboro GO, Alhassan AJ, Owolarafe TA, Ononamadu CJ and Sule MS. Evaluation of the biosafety potentials of *Tapinanthus bangwensis* and *Moringa oleifera* leaves using *Allium cepa* Model. Toxicol Reports 2020b;7: 671-679.

15. Ihegboro GO, Ononamadu CJ, Ihegboro SN and Jeph-Rolland IC. Reversibility of the Biochemical Abnormality linked to CCl4-induced Hepatotoxicity by extracts/fractions of *Tapinanthus bangwensis* and *Moringa oleifera* leaves. Sci J. Appl Natr Sci 2023;2(1):59-69.

16. Ihegboro GO, Ononamadu CJ, Owolarafe TA and Shekwolo I. Screening for toxicological and anti- diabetic potential of n-hexane extract of *Tapinanthus bangwensis* leaves. Toxicol. Res. Application, 2020a;4:1-11.

17. Ihegboro GO, Ononamadu CJ, Owolarafe TA, Mujiburrahman F and Okoro EJ. Anti-reno-hematological tenacity of *Calotropis procera* aqueous-methanol root extract in Alloxan-induced Pancrotoxic Wistar rats. Comparative Clin. Pathol 2022;1-9.

18. Ihegboro GO, Ononamadu CJ, Owolarafe TA, Olayinka O, Udeh JJ, Saliu AO, Abolaji DD,

19. International Diabetes Federation. *Diabetes Atlas* (10th ed.). Brussels, Belgium. 2021.

20. Mahnashi MH, Alqahtani YS, Alyami BA, Alqarni AO, Ayaz M, Ghufra M, Ullah F, Sadiq, A, Ullah I, Haq IU, Khalid M and Murthy HCA. Phytochemical Analysis, α-Glucosidase and Amylase Inhibitory, and Molecular Docking Studies on *Persicaria hydropiper L.* Leaves Essential Oils. Evidence-Based Complementary and Alternative Med. 2022;10:1155.

21. Meng XY, Zhang HX, Mezei M and Cui M. Molecular docking: A powerful approach for structure-based drug discovery. Curr. Computer Aided Drug Des 2011;7(2):146-157.

22. Mohiuddin GS, Palaian S, Shankar PR, Sam KG, and Kumar M. Uncommon side effects of commonly used anti-diabetics: Time to monitor them. Int. J. Pharm Sci and Res 2019;10(9): 4145-4148.

23. Mustafa G, Mahrosh HS, Zafar M, Attique SA, Arif R. Exploring the antihyperglycemic potential of tripeptides devised from AdMcl via different receptor proteins inhibition using in silico approaches. International J. Immunopathol and Pharmacol 2022;36(1):1-11.

24. Natarajan A, Gugumar S, Bitragunta, S and Balasubramanyan N. Molecular docking studies of (4 Z, 12 Z)-cyclopentadeca-4, 12-dienone from *Grewia hirsuta* with some targets related to type 2 diabetes. BMC complementary and alternative Med. 2015;15(1):1-8.

25. Ononamadu CJ, and Ibrahim A. Molecular docking and prediction of ADME/drug-likeness properties of potentially active antidiabetic compounds isolated from aqueous-methanol extracts of *Gymnema sylvestre* and *Combretum micranthum*. *BioTechnologia* J. Biotechnology, Computational Biology and Bionanotechnology 2021;102 (1): 85–99.

26. Ononamadu CJ, Mohmad A and Ihegboro GO. Uncovering the potential novel antidiabetic compounds from African medicinal plants: A computer-Aided study. Avicema J Med Biochem 2024;12(2): 77-92.

27. Pankaj S, Manvender S, Sangeeta S. Molecular docking analysis of pyruvate kinase M2 with a potential inhibitor from the ZINC database. Biomedical informatics 2021;17(1):139-146.

28. Qui X, Ren L, Yang X, Bai F, Wang L, Geng P, Bai G, Shen Y. Structure of pancreatic alpha amylase in complex with

acarviostatins: Implications for drug design against Type 2-diabetes. J. Structural Biol 2011;174(1):196-202.

29. Rohmah J. Antioxidant activities using DPPH, FIC, FRAP, and ABTS methods from ethanolic extract of *Lempuyang Gajah* Rhizome. Jurnal Kimia Riset 2022;7(2):152-166

30. Safitri A, Fatchiyah F, Sari DR and Roosdiana A. Phytochemical screening, in vitro anti-oxidant activity, and in silico anti-diabetic activity of aqueous extracts of *Ruellia tuberosa* L. J. Applied Pharmaceutical Sci 2020;10(3):101-8.

31. Savjani KT, Gajjar AK, Savjani JK. Drug solubility importance and enhancement techniques. ISRN Pharm 2012;195727:1-10.

32. Smita K, Manjunath K, Sarangi S. Evaluation of α-glucosidase inhibitory potential of methanolic leaf extract of *ocimum canum.* International J. pharmacy and pharmaceutical Sci 2018; 10(1):126-131.

33. Vignesh A, Selvakumar S and Vasanth K. Comparative LC-MS analysis of bioactive compounds, antioxidants and antibacterial activity from leaf and callus extracts of *Saraca asoca.* Phytomedicine Plus 2022;2:100167.

34. Yixin R, Li L, Li W, Yan H, Shuang C. Glucokinase as an emerging antidiabetes target and recent progress in the development of its agonists. J. Enzyme Inhib Med Chem 2022;37(1):606-615.